

https://dspace.org/

Impact of Metal Oxide Nanoparticles in Waste Plastic Oil on Diesel Engine Performance Combustion Emissions and Tribology

Arunprasad Jayaraman; Michael Atkins

ASME
https://hdl.handle.net/10539/45585
WOS

Downloaded from a DSpace repository. https://dspace.org/

Check for updates

Journal of Energy Resources Technology, Part A: Sustainable and Renewable Energy
asmedigitalcollection.asme.org | Journal archive available at: https://asmedigitalcollection.asme.org/energyresources

Impact of Metal Oxide Nanoparticles in Waste Plastic Oil on Diesel Engine Performance, Combustion, Emissions, and Tribology

J. Arunprasad[1]
School of Mechanical, Industrial and Aeronautical Engineering,
University of the Witwatersrand,
Johannesburg 2000, South Africa
e-mail: a0086458@wits.ac.za

Michael D. Atkins
School of Mechanical, Industrial and Aeronautical Engineering,
University of the Witwatersrand,
Johannesburg 2000, South Africa
e-mail: michael.atkins@wits.ac.za

The study explores the potential of waste plastic oil (WPO) as a sustainable alternative fuel, aiming to enhance engine performance and emission characteristics by incorporating zinc oxide (ZnO) nanoparticles. The ZnO nanoparticles were characterized by scanning electron microscopy (SEM), transmission electron microscopy (TEM), and energy-dispersive X-ray analysis. Using an ultrasonicator, they were dispersed in WPO20 blends at 30, 60, 90, and 120 ppm concentrations. Engine experiments conducted at 1500 rpm revealed that the WPO20 blend with 120 ppm ZnO exhibited a 23.53% increase in cylinder pressure and a 12.5% enhancement in heat release rate compared to WPO20. The brake thermal efficiency (BTE) of WPO20 + 120 ppm ZnO improved by 6.54%, while brake-specific fuel consumption (BSFC) decreased by 16.02%. Emission analysis showed reductions in carbon monoxide (CO), hydrocarbons (HCs), and smoke opacity by 14.86%, 35.71%, and 12.5%, respectively, with a slight 2.65% rise in nitrogen oxide (NO_x) emissions compared to WPO20 at peak load. Tribological evaluations using a four-ball tribometer demonstrated significant improvements, including a 20.79% reduction in the coefficient of friction (COF), a 28.09% decrease in wear scar diameter (WSD), and a 58.65% enhancement in the flash temperature parameter (FTP) compared to WPO20. SEM analysis of worn surfaces confirmed reduced wear and surface damage in blends containing ZnO nanoparticles, with WPO20 + 120 ppm ZnO exhibiting superior overall performance in both engine and tribological tests.
[DOI: 10.1115/1.4068582]

Keywords: waste plastic oil, zinc oxide, performance, combustion, emission, tribology

1 Introduction

The rapid growth in industry, transportation, and mobile lifestyles has significantly increased global energy demand [1]. This surge in energy consumption, coupled with a rising global population, has led to higher demand and prices for petroleum-based fuels [2]. The growing interest in alternative fuels is a response to these pressing challenges [3]. Plastic has become an integral part of our everyday lives, particularly in the form of single-use items. The amount of plastic produced worldwide has increased dramatically, from 275 MT in 2012 to 460 MT in 2019. At this alarming rate, it could reach a staggering 1231 MT by 2060 [4]. Disposing of this plastic has become a significant environmental issue [5]. In response to this crisis, researchers have investigated the conversion of discarded plastic into waste plastic oil (WPO) through a pyrolysis process [6]. This method not only serves as an alternative source of energy but also helps reduce plastic waste [7]. The double-bonded carbon structures and aromatic groups in plastic oil limit its blending ratio with diesel, as these features can negatively impact fuel compatibility. Meanwhile, the high aromatic content of waste plastic oil contributes to increased emissions. Its high viscosity, elevated density, and low volatility further complicate its use, raising concerns about fuel stability and efficient combustion [8–11]. Due to the complex design of diesel engines, making structural changes can be challenging [12,13]. As a result, using fuel blends and nanoparticles is often a more accessible and cost-effective approach to improve performance, combustion, and lower emissions. Due to their growing popularity, nanoparticles are frequently used in waste plastic oil. These nanoparticle additives have garnered significant attention within the energy and transportation sectors for their potential to enhance fuel performance and efficiency. Extensive research suggests incorporating nanoparticles can improve fuel characteristics, leading to more efficient combustion and enhanced engine performance. The most often used nanoparticles include CeO_2, ZnO, MgO, La_2O_3, TiO_2, CuO, Al_2O_3, and carbon nanotube [14–18]. This improvement in fuel performance can be attributed to the nanoparticles' large surface area relative to their volume and superior capacity for heat and mass transfer. In

[1]Corresponding author.
Manuscript received November 27, 2024; final manuscript received April 22, 2025; published online May 19, 2025. Assoc. Editor: Vittorio Ravaglioli.

Copyright © 2025 by ASME

Downloaded from http://asmedigitalcollection.asme.org/energyresourcesrenewable/article-pdf/1/5/051503/7492444/jerta-24-1207.pdf by University of Witwatersrand - Warteweiler Library user on 20 May 2025

addition, their catalytic properties help to reduce emissions. Compared to other metal oxide nanoparticles, ZnO particles possess unique properties, including high surface energy, strong adsorption, excellent chemical stability, and distinctive electrical, optical, and tribological characteristics. Likewise, ZnO offers a large surface area, high diffusion rates, and antimicrobial activity. In addition, ZnO is nontoxic, environmentally friendly, cost-effective, and biocompatible [19,20].

Table 1 compares the effects of different metal oxide nanoparticles containing plastic oil blends on engine performance, combustion, and emissions [21–29]. Transforming waste plastics into lubricating oils presents a promising solution for machinery lubrication, offering a viable alternative to traditional oils. Waste plastic-derived oils can effectively act as lubricants, reducing friction and wear in machinery components due to their composition. In contrast, petroleum-based lubricants release carbon into the environment, increasing surface carbon levels and disrupting the carbon cycle. Several researchers focus on alternative resources for producing lubricants that minimize environmental harm. By using a four-ball tribometer, they analyzed waste tire pyrolysis oil's friction and wear characteristics as a lubricant and compared it with diesel and biodiesel. The findings indicated that the coefficient of friction (COF) for waste tire plastic oil was 22.3% less than diesel and 10.6% less than biodiesel, with smaller worn surfaces observed [30]. They conducted tribology experiments using a four-ball tribometer to study waste plastic oil's friction and wear characteristics in combination with synthetic lubricant at 15% and 30% concentrations. The results revealed that the synthetic lubricant that contains 30% waste plastic oil exhibited the lowest frictional coefficient, smaller wear scar diameter, improved wear morphology, and increased viscosity than the other lubricants [31].

Furthermore, incorporating nanoparticles can enhance the performance and efficiency of lubricants. These nanoparticles extend the range of applications by enhancing thermal stability and antiwear properties. Their small size enables them to penetrate contact zones effectively, enhancing lubrication [32,33]. Nanoparticles create a protective tribofilm on contact surfaces that reduces friction and wear, acting as highly efficient nanolubricants to improve the overall performance of the lubricant [34]. Several studies have investigated ways to improve the performance of these lubricants, with nanoparticles playing a significant role in enhancing their tribological properties. Table 2 illustrates the comparative analysis of the tribology performance of pyrolysis oils with different nanoparticles [35–38]. The comprehensive literature review underscores the notable potential of metal oxide nanoparticle blends in enhancing wear resistance and reducing friction. Also, the literature review reveals limited research on using metal oxide nanoparticles in waste plastic oil.

This study presents an innovative approach to enhancing waste plastic oil with zinc oxide nanoparticles, addressing the dual challenges of plastic waste management and the demand for renewable energy. Comprehensive characterization of ZnO nanoparticles was performed using advanced techniques such as scanning electron microscopy (SEM), transmission electron microscopy (TEM), and energy-dispersive X-ray spectroscopy (EDX), providing detailed insights into their structural and compositional properties. The research evaluates the effects of various fuel blends, including pure diesel, WPO20 (80% diesel and 20% waste plastic oil), and WPO20 enhanced with ZnO nanoparticles at concentrations of 30, 60, 90, and 120 ppm, on engine performance, combustion, and emission characteristics. Additionally, a four-ball tribometer was employed to analyze the friction and wear behavior of WPO with ZnO nanoparticles, offering a thorough understanding of its tribological properties.

2 Materials and Methods

2.1 Conversion of Waste Plastics Into Oil. The current study concentrated on low-density polyethylene plastic, used as the primary raw material, to investigate its potential for producing alternative fuels. Pyrolysis is a thermal decomposition process that decomposes organic materials into smaller molecules by applying heat without oxygen [39]. This process converts biomass and other feedstocks into valuable products such as bio-oil, gas, and char, which can be used for energy generation or as feedstock for chemical production [40]. The collected plastic waste is first sorted to remove nonrecyclable materials. The recyclable plastic is then shredded into smaller pieces using a waste plastic cutting machine. The plastic waste is first cut into small pieces, typically 1–2 cm^2, using a cutting machine. These smaller, uniformly sized pieces are loaded into a fixed bed reactor. The smaller particle size enhances the efficiency of the thermal decomposition process, ultimately leading to a higher oil yield. In the case of shredded plastic, it is heated in an oxygen-free environment, causing it to decompose into more minor hydrocarbon (HC) compounds, producing liquid plastic oil, gaseous, and solid byproducts like char. Figure 1 illustrates the schematic representation of a pyrolysis plant comprising a reactor and a condenser. This is the laboratory-scale plant. The reactor features a stainless steel drum with a diameter of 1300 mm, insulated with a thin sheet. The unit features three 1500 W electrical heating coils that warm the reactor walls. The thin sheet and the reactor are separated by a layer of glass wool for insulation. The reactor setup consists of several key components, including a mechanical stirrer with a motor housing, a control valve, and a pressure gauge. It also features a feed hopper with a control valve, a K-type thermocouple for temperature measurement, a hand hole for manual access, a control panel for operation management, and a safety valve. The temperature was maintained at 550 °C for 30 min under isothermal conditions, with a heating rate of 20 °C per minute from ambient temperature. Temperatures are monitored using thermocouples and displayed on a control panel indicator, which the controller operates. During pyrolysis, a hand hole with a stopcock is situated at the bottom of the reactor, allowing for the removal of approximately 20–25% of the waste material after it has undergone pyrolysis. The condensers comprise cooling coils and water containers connected to the reactor outlets to condense plastic vapor. The cooling coil is made of stainless steel, with a total length of 1800 mm and an inner diameter of 20 mm. The container housing the coil measures 500 mm in height and has a diameter of 300 mm. There are two valves for proportioning and returning water in this sink. The pyrolysis liquid is stored in a corrosion-resistant stainless steel fuel accumulator, and the spraying takes 3.5 h. AVL 444 Di Gas analyzer measures unburned hydrocarbon emissions as uncondensed gases passing through the flame arrester. Here, water is utilized to prevent the possibility of backfires. The uncondensed gas is supplied to the burner at the end, where the waste is burned, producing a blue flame that cleans the air. Briefly, the distillation unit fractionates the denatured liquid from the pyrolysis plant and produces waste oil from plastic. From 1 kg of waste plastic, the process generated 690 g of plastic oil, accounting for 69% of the total weight, 7% by weight of gaseous fractions, and 24% of solid coke residue.

2.2 Characterization of ZnO Nanoparticles. The zinc oxide nanoparticles were thoroughly characterized utilizing a TESCAN OXFORD scanning electron microscope and energy-dispersive X-ray analysis. The scanning electron microscope was in an acceleration voltage range of 15–20 kV, offering magnification capabilities from 1000× to 100,000×, and employed VEGA 3 INCA software for image acquisition and elemental mapping. ZnO nanoparticles were examined using an analytical electron microscope, JEM-2100, operating at 200 kV.

2.3 Fuel Preparation. The fuel preparation process flow is shown in Fig. 2. The WPO20 fuel blend was prepared using a magnetic stirrer. The zinc oxide nanoparticles (Sigma Aldrich,

Downloaded from http://asmedigitalcollection.asme.org/energyresourcesrenewable/article-pdf/1/5/051503/7492444/jerta-24-1207.pdf by University of Witwatersrand - Warteweiler Library user on 20 May 2025

Table 1 The impact of different metal oxide additives on the performance, combustion, and emission characteristics of waste plastic oil with different nanoparticles

Sample and nanoparticle /testing samples	SEM/TEM/EDX	Testing conditions	HRR (%)	CP (%)	ID (%)	SFC (%)	BTE (%)	CO (%)	Smoke (%)	HC (%)	NO_X (%)	References
Waste plastic oil blends (ULDP20) and graphene quantum dot 1. Diesel 2. ULDP20 (**Reference**) 3. ULDP20G30 4. ULDP20G40 5. ULDP20G50	NA	4.4 kW at 1500 rpm/23 deg CA BTDC/ 200 bar	49.8 J/deg CA for ULDP 20	59.3 bar for ULDP20	7.29 deg CA for ULDP 20	▼ 6.85	▲ 5.71	▼ 7.04	▼ 2.33	▼ 3.71	▼ 1.63	[21]
Waste cable pyrolysis oil (WCPO) and boron oxide (B_2O_3) 1. Diesel (**Reference at 3000 rpm**) 2. WCPO20 3. **WCPO20 + B_2O_3/0 ppm**[a] 4. WCPO20 + B_2O_3/40 ppm 5. WCPO20 + B_2O_3/60 ppm From RSM methods: Engine load: 1500 W, B_2O_3: 22 ppm[a]	SEM	7 Hp at 3000 rpm	NA	NA	NA	▼ 12.3	▲ 14.1	▼ 18.3	NA	▼ 16.1	▲ 4.31	[22]
Waste plastic oil and zinc oxide (ZnO) 1. WPO20 (**Reference**) 2. WPO20ZnO50 3. **WPO20ZnO100**[a] 4. WPO20ZnO150	XRD/TEM — 45.89 nm/ spherical	5.2 kW 1500 rpm/23 deg CA BTDC/17.5:1	NA	NA	NA	12.8 ▼	2.47 ▲	5.7 ▼	11.8 ▼	28 ▼	14.9 ▼	[23]
Waste plastic oil and magnesium oxide (MgO) 1. Diesel 2. PPO (**Reference**) 3. PPO + 25MNA 4. PPO + 50MNA 5. **PPO + 75MNA**[a] 6. PPO + 100MNA	XRD — 30 to 40 nm/ SEM — 20 nm/EDX	5.2 kW at 1500 rpm/23 deg CA BTDC/17.5:1	24 ▲	1.20 ▲	—	12.5 ▼	7.93 ▲	0.03 by vol ▼	11.9 ▼	4.28 ▼	3.06 ▲	[24]
Neat plastic oil and titanium oxide (TiO_2) 1. PO (**Reference**) 2. POAL100 3. POAL150 4. **POAL200**[a]	—	17.5:1	—	3.5 ▲	—	—	—	51.1 ▼	—	15.0 ▼	—	[25]
Plastic oil and titanium oxide (TiO_2) 1. Diesel 2. PO (**Reference**) 3. POAL100 4. POAL150 5. **POAL200**[a]	SEM — 15 and 22 nm	3.7 kW at 1500 rpm/23 deg BTDC/17:1	9.9 ▲	3.4 ▲	—	—	2.6 ▲	45.4 ▼	150 ppm TiO_2 NPs 38 ▼	18 ▼	5.2 ▲	[26]
Plastic pyrolysis oil and titanium oxide (TiO_2)	XRD –	5.2 kW at	23.8 ▲	—	—	12.5 ▼	2.1 compared to	66% PPO + 100 ppm	1 ▼	6 ▼	PPO + 100 ppm	[27]

Downloaded from http://asmedigitalcollection.asme.org/energyresourcesrenewable/article-pdf/1/5/051503/7492444/jerta-24-1207.pdf by University of Witwatersrand - Wartewelier Library user on 20 May 2025

Table 1 *Continued*

Sample and nanoparticle /testing samples	SEM/TEM/EDX	Testing conditions	HRR (%)	CP (%)	ID (%)	SFC (%)	BTE (%)	CO (%)	Smoke (%)	HC (%)	NO_X (%)	References
1. Diesel	30 to 40 nm/	1500 rpm /20 deg					diesel	TiO_2			TiO_2	
2. PPO (**Reference**)	SEM — 30 to	CA BTDC/17.5:1					▲	▼			6.38 at ▲	
3. PPO + 25 ppmTiO_2	40 nm/EDS/											
4. **PPO + 50 ppmTiO_2** [a]	FTIR											
5. PPO + 75 ppmTiO_2												
6. PPO + 100 ppmTiO_2												
Neat plastic oil and alumina	SEM	3.7 kW at	2	3.5	27.2	9.1	10.3	55.6	33	62.3	7.7	[28]
1. Diesel	—	1500 rpm/23 deg	▲	▼	▼	▼	▲	▼	▼	▼	▼	
2. PO (**Reference**)	45 to 65 nm	BTDC/16:5										
3. PAN100												
4. PAN150												
5. **PAN200** [a] (100, 150, and 200 mg/L)												
Waste plastic oil and cerium oxide (CeO_2)	—	1500 rpm/16.5:1	—	—	—	32.4	27.7	B50 + CeO_2	▼	B50 + CeO_2	B50 + CeO_2	[29]
						▼	▲	50 ppm		50 ppm/	50 ppm/	
								0.02 ppm		19 ppm	53 ppm	
								▼		▼	▼	

[a]Bold indicates base and best samples.

[a]Note: CP: Cylinder pressure; EDS: Energy dispersive X ray test; SFC: Specific fuel consumption, RSM-Response surface methodology; XRD: X ray diffraction.

Bangalore, India) were then incorporated into the waste plastic oil through ultrasonication. An ultrasonicator, operating at 120 watts and 40 kHz, was used to uniformly disperse the ZnO nanoparticles throughout the waste plastic oil over 45 min to achieve a homogeneous mixture. Ultrasonication was used to evenly distribute ZnO nanoparticles in the WPO20 blend at 30, 60, 90, and 120 ppm concentrations. The test fuels produced were designated as WPO20 + 30 ppm ZnO, WPO20 + 60 ppm ZnO, WPO20 + 90 ppm ZnO, and WPO20 + 120 ppm ZnO. The physicochemical properties of the WPO20-ZnO nanoparticle blend, evaluated according to ASTM standards, are presented in Table 3. Using nanoparticle catalysts reduces the activation energy for combustion, enhancing fuel molecule decomposition and oxidation, thus facilitating combustion, improving efficiency, and elevating the calorific value [41].

2.4 Experimental Setup and Methodology. The experimental setup is shown schematically in Fig. 3. This study used a Kirloskar four-stroke, water-cooled direct injection diesel engine with a single cylinder and four strokes. In the testing engine, 1500 revolutions per minute were rotated at maximum, delivering 5.2 kW of power. It featured a water jacket system designed to regulate wall temperatures by circulating coolant around the combustion chamber. Key engine specifications included a displacement of 661cc, a compression ratio 17.5:1, and fuel injection timing of 23 deg before the top dead center at an injector pressure of 210 bar. Fuel flow, air flow, fuel consumption, and cylinder pressure were recorded using a data acquisition system connected to various parts of the experimental test rig. The data acquisition system is integrated with a computer running "ENGINE SOFT" software to collect combustion parameters, performance characteristics, and cylinder pressure during combustion. This data collection device is connected to all relevant sensors, enabling the real-time display of the gathered information on a personal computer. Emissions and smoke levels were measured using the AVL 444N DiGas analyzer and AVL smoke meter. Baseline performance data were first collected with the engine running on diesel fuel at 1500 rpm under no-load conditions for 30 min, with cooling water and lubricating oil temperatures maintained constant. The performance of various test fuels was evaluated by analyzing metrics such as brake thermal efficiency (BTE), brake-specific fuel consumption (BSFC), cylinder pressure, heat release rate, and emissions (carbon monoxide (CO), HC, smoke opacity, and nitrogen oxide (NO_x)) under load conditions ranging from 0% to 100%. Three trials were conducted for every test, and the mean values were recorded. Table 4 presents the engine's technical specifications.

2.5 Four-Ball Tribometer. Under controlled conditions, the four-ball tribometer is a versatile testing device used to examine the tribological characteristics of lubricants and materials, such as friction, wear, and lubrication performance. The current research utilized a TR-30L-IAS four-ball tribometer. This device operates by placing four steel balls in contact, three stationary and one rotating, allowing for accurate measurement of parameters such as wear scar diameter, coefficient of friction, and frictional torque. Figure 4 depicts a visual representation of the experimental setup for the four-ball tribometer. Before testing, the steel balls and the oil cup underwent a thorough cleaning process utilizing toluene to ensure the removal of any residual contaminants. After cleaning, the bottom steel balls were placed inside the oil cup. The collet launched a single steel ball through the machine. Specimen balls measuring 1/2 in. in diameter and 1 in. in thickness were prepared according to the ASTM-D4172 standards. The specimens were fabricated from chrome alloy steel that met the AISI E-52100 Grade 25 EP (Extra Polish) standard, with a Rockwell hardness between 64 and 66 on the C scale. All specimens were thoroughly cleaned using an ultrasonic bath sonicator immersed in ethanol for 5 min, with a fresh wipe used only once. The oil cup was filled with 10 ml of test fuel during the test, ensuring the complete coverage of the three test balls. The testing was carried out at a consistent

Downloaded from http://asmedigitalcollection.asme.org/energyresourcesrenewable/article-pdf/1/5/051503/7492444/jerta-24-1207.pdf by University of Witwatersrand - Warteweiler Library user on 20 May 2025

Table 2 Tribology characteristics of pyrolysis oil with different nanoparticles

Sample and nanoparticles/testing samples	SEM/ TEM/ XRD/ EDX	Tribological experiment/operating conditions	COF (%)	WSD (%)	FTP (%)	Roughness (%)	Worn surface analysis	References
Filtered tire pyrolysis oil (MgO, graphene, Al_2O_3) 1. PB20FTPO10 **(Reference)** 2. MgO: 0.1% 3. **MgO: 0.2%** [a] 4. G: 0.1%, 5. G: 0.2%, 6. **Al_2O_3: 0.1%** [a] 7. Al_2O_3: 0.2%	NA	Four-ball tribo-tester, ASTM-D4172 Load: 40 kg Speed: 1200 rpm Temperature; 75 °C Time: 10 min	Al_2O_3 — 0.1% ▼ 2.83	Al_2O_3 — 0.1% ▼ 22.09	NA	MgO: 0.2% ▼ 36.9	SEM/EDX	[35]
Plastic oil and graphene nanoplatelets (GNPs) and hexagonal boron nitride (hBN) 1. PO **(Reference)** 2. PO + 0.5% GNP 3. PO + 1.0% GNP **4. PO + 1.5% GNP** [a] 5. PO + 2.0% GNP 6. PO + 0.5% hBN 7. PO + 1.0% hBN 8. PO + 1.5% hBN	NA	A ball on disk	54 ▼	85 ▼	NA	NA	Raman spectra analysis	[36]
Waste plastic oil (PO) and CuO 1. PO **(Reference)** 2. **PO + 0.5% CuO** [a] 3. **PO + 1.0% CuO** [a] 4. PO + 1.5%CuO 5. Mineral oil	SEM/ XRD	A ball on disk	PO + 1.0% CuO ▼ 20	PO + 0.5% CuO ▼ 44	NA	NA	SEM/EDX	[37]
Waste PO and GNP and hBN 1. PO **(Reference)** **2. PO + 0.5% GNP** [a] 3. PO + 1.0% GNP 4. PO + 1.5% GNP 5. PO + 2.0% GNP **6. PO + 0.5% hBN** [a] 7. PO + 1.0% hBN 8. PO + 1.5% hBN 9. PO + 2.0% hBN	SEM	A ball on disk	**PO + 0.5% hBN** ▼ 63	**PO + 0.5% GNP** ▼ 3	NA	NA	SEM/EDX/ Raman spectra analysis	[38]

[a]Bold indicates base and best samples.
XRD: X ray diffraction.

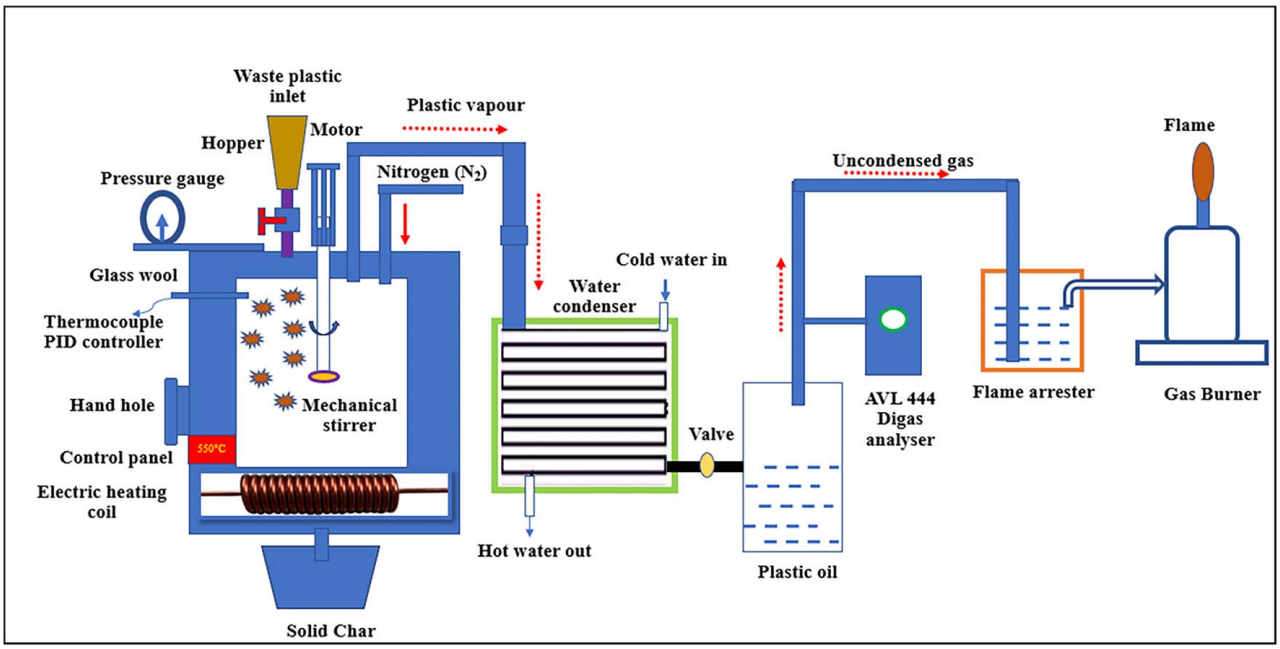


Fig. 1 Schematic diagram of pyrolysis plant

Downloaded from http://asmedigitalcollection.asme.org/energyresourcesrenewable/article-pdf/1/5/051503/7492444/jerta-24-1207.pdf by University of Witwatersrand - Warteweiler Library user on 20 May 2025

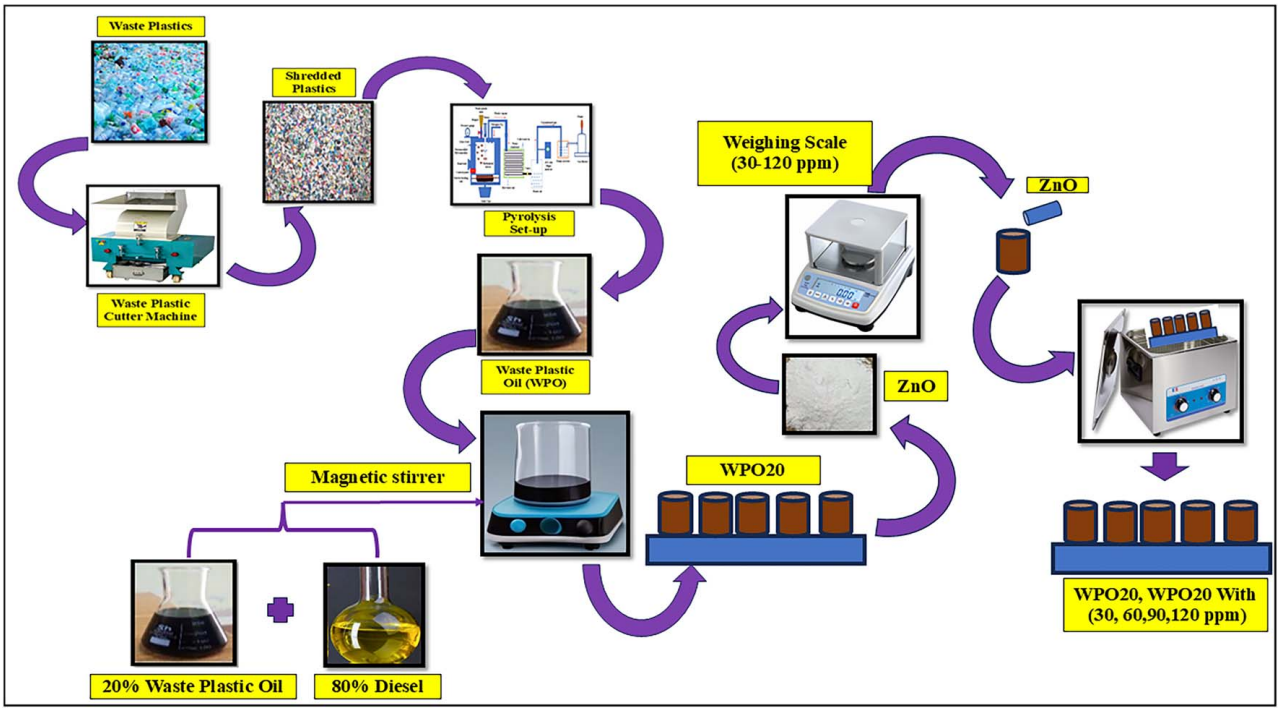


Fig. 2 The outline of fuel preparation processes

shaft speed of 1200 revolutions per minute, a constant temperature of 75 °C, and a load of 40 kg for a duration of 3600 s.

2.5.1 Coefficient of Friction. The four-ball tribometer was connected to a computer equipped with WINDUCOM 2010 software, which recorded and measured the friction torque and coefficient of friction. The coefficient of friction was calculated based on the frictional torque, as outlined in Eq. (1):

$$\mu = \frac{T \times \sqrt{6}}{r \times 3w} \tag{1}$$

where T represents the frictional torque, expressed in kg · mm; W represents the applied weight in kg, and the contact surface of the spheres is located 3.67 mm perpendicularly from the axis of rotation, with this distance represented by r.

2.5.2 Wear Scar Diameter. The wear scar diameter of the three test balls was measured using an optical microscope with a 0.01 mm resolution to assess the lubricant's effectiveness.

2.5.3 Flash Temperature Parameter. Flash temperature is one of the most important parameters that protect the machinery of a lubricant against wear and damage during high-pressure and high-temperature conditions. When the flash temperature parameter (FTP) value is maximum, it protects the contact surfaces from wear and damage. The formula is often used to calculate the FTP value.

$$\text{FTP} = (\text{axial load in kg})/(\text{wear scar diameter in mm})^{1.4}$$

3 Results and Discussion

The present study investigates how blending waste plastic oil with ZnO nanoparticles influences engine performance, combustion, and emissions characteristics. The primary fuel blend comprises 20% waste plastic oil and 80% diesel by volume, with zinc oxide nanoparticles incorporated at 30–120 ppm concentrations. The experimental investigation was conducted at various fuel blend compositions while maintaining a constant engine speed of 1500 revolutions per minute. The findings of the experimental study and a detailed analysis of the observed outcomes are presented in the subsequent sections.

3.1 The Morphology of Zinc Oxide Nanoparticles. The scanning electron microscope was operated at a magnification of 10,000X and a potential of 20 kV, as shown in Fig. 5. In Fig. 5(*a*), visual examination using the SEM revealed the presence of possible zinc oxide nanoparticles and aggregated particles. The ZnO nanoparticles exhibited a spherical shape. The transmission

Table 3 Physicochemical properties of various fuel blends

Property	Method	Diesel	WPO20	WPO20 + 30 ppm ZnO	WPO20 + 60 ppm ZnO	WPO20 + 90 ppm ZnO	WPO20 + 120 ppm ZnO
Density at 15 °C, kg/m^3	ASTM D4052	830	0.763	0.782	0.809	0.824	0.828
Kinematic viscosity at 40 °C	ASTM D445	3.12	3.31	3.26	3.09	2.84	2.72
Calorific value (kJ/kg)	ASTM D240	42,500	41,387	41,780	41,912	42,193	42,271
Flashpoint (°C)	ASTM D93	58	62	62	56	53	51
Cetane number	ASTM D4737	51	30	31	34	36	39

Downloaded from http://asmedigitalcollection.asme.org/energyresourcesrenewable/article-pdf/1/5/051503/7492444/jerta-24-1207.pdf by University of Witwatersrand - Warteweiler Library user on 20 May 2025

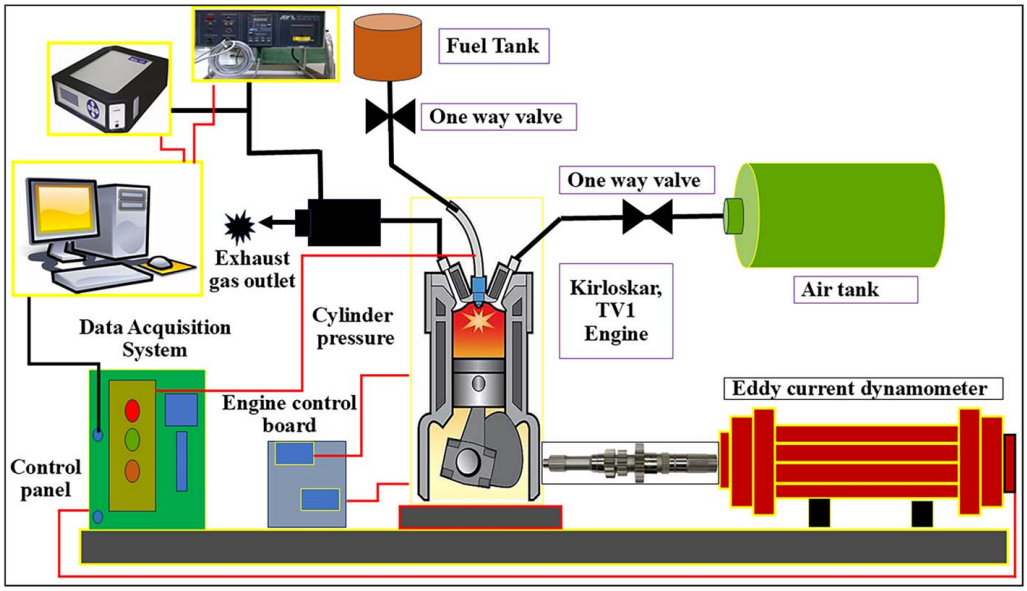


Fig. 3 Schematic illustration of engine experimental setup

electron microscopy analysis in Fig. 5(*b*) revealed that the zinc oxide nanoparticles possessed a size range extending from 31 to 49 nm. The existence of ZnO nanoparticles was confirmed through energy-dispersive X-ray analysis, with the elemental composition indicated by the relevant peaks in the EDX mapping. Prominent peaks at 0.5 keV and 1 keV in the EDX analysis confirm the presence of elements in the ZnO nanoparticle. The EDX spectrum in Fig. 5(*c*) discovered the weight percentages of Zn (46.14%), C (23.93%), and O (29.93%).

3.2 Cylinder Pressure. Cylinder pressure depends on the fuel, engine type, and air–fuel ratio. The cylinder pressure is determined by analyzing data collected from a data acquisition system, which measures fluctuations in pressure and volume during crankshaft rotation. The software "ENGINE SOFT" collects data from a pressure sensor connected to a computer. Figure 6(*a*) shows the fluctuation in in-cylinder pressure for different fuel blends under peak load conditions. The findings indicated that, under full-load conditions, the cylinder pressures for diesel, WPO20, WPO20 + 30 ppm ZnO, WPO20 + 60 ppm ZnO, WPO20 + 90 ppm ZnO, and WPO20 + 120 ppm ZnO were 72.47 bar, 58.2 bar, 64.05 bar, 69.01 bar, 71.38 bar, and 71.85 bar, respectively. Based on the outcomes, the diesel blend exhibited the maximum cylinder pressure, whereas the WPO20 blend showed a comparatively lower pressure than the other tested blends. In comparison with diesel, the percentage decreases in-cylinder pressure was 19.69% for WPO20, 11.63% for WPO20 with 30 ppm ZnO, 4.77% for WPO20 with 60 ppm ZnO, 1.5% for WPO20 with 90 ppm ZnO, and 0.85% for WPO20 with 120 ppm ZnO. Adding ZnO nanoparticles to WPO20 blends enhances cylinder pressure due to the improved thermal conductivity of the nanoparticles. At maximum load, the blends WPO20 + 30 ppm ZnO, WPO20 + 60 ppm ZnO, WPO20 + 90 ppm ZnO, and WPO20 + 120 ppm ZnO showed cylinder pressure increases of 10.06%, 18.57%, 22.56%, and 23.53%, respectively, compared to WPO20. This improvement has led to more effective fuel–air mixing and a faster combustion process, significantly boosting the engine's power output. Supporting our findings, other studies have

Table 4 Technical specification of engine

Title	Detail
Manufacturer and model	Kirloskar, TV1, 4-Stroke
No. of cylinders	1
Speed (rpm)	1500
Compression ratio	17.5:1
Ignition timing	23 deg BTDC
Rod length (mm)	234
Displacement volume (cc)	661.45
Rated output (kW)	5.2
Injection pressure (bar)	210
Cooling method	Water- cooled
Lubricating oil	SAE40
Maximum brake power (kW)	5.2
Bore and stroke (mm)	87.5 & 110
Injection type	Direct
Flywheel diameter (mm)	1262
Load cell	Liquid-cooled eddy current dynamometer
Dynamometer arm length (mm)	185
Orifice diameter mm	20
Piezo sensor	Design PCB, USA Combustion, and diesel line, capable of handling pressures up to 350 bar while incorporating low-noise cable
Crank angle sensor	1 deg resolution, capable of speeds up to 5500 rpm, with top dead centre pulse detection

Downloaded from http://asmedigitalcollection.asme.org/energyresourcesrenewable/article-pdf/1/5/051503/7492444/jerta-24-1207.pdf by University of Witwatersrand - Warteweiler Library user on 20 May 2025



Fig. 4 Illustration of the four-ball tribometer test setup

demonstrated that adding graphene oxide nanoparticles to fuel mixtures can greatly enhance combustion efficiency. The high surface area-to-volume ratio of ZnO nanoparticles enhances heat exchange between the nanoparticles and fuel droplets, improving combustion efficiency and resulting in more thorough and efficient combustion as cylinder pressure increases with the incorporation of nanoparticle blends [42].

3.3 Heat Release Rate. The heat release rate, an important combustion characteristic, is determined from the in-cylinder gas pressure. This metric can be used to describe different combustion phases. The general equation for the heat release rate in thermodynamics, particularly for combustion processes, is derived from the first law of thermodynamics and energy conservation principles. By excluding crevice effects, the rate of heat emission can be determined using an appropriate heat release analysis equation [2]. The heat release rate during combustion is measured using the following equation:

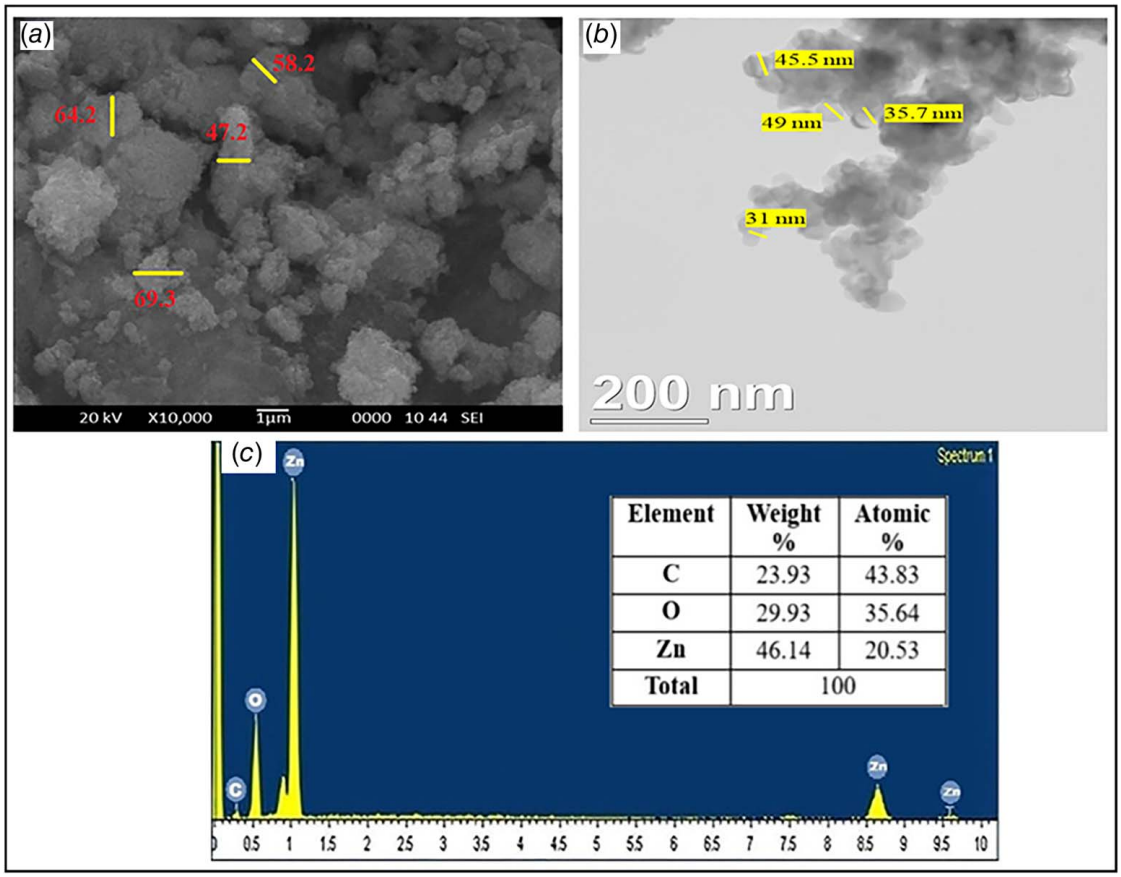
$$\frac{dQ_n}{d\theta} = \frac{\gamma}{\gamma - 1} P \frac{dV}{d\theta} + \frac{1}{\gamma - 1} V \frac{dP}{d\theta} \tag{2}$$

Here, the variables P, V, and θ refer to cylinder pressure, volume, and engine crank angle in the combustion equations for a diesel engine. Meanwhile, γ denotes the specific heat ratio within the cylinder. The heat release rate during the premixed combustion phase in the engine's combustion chamber is affected by several important factors. These include the ignition delay, the air–fuel mixing rate, and the fuel's calorific value. These parameters are crucial in determining the overall combustion dynamics and efficiency within the engine's operating cycle. Analyzing the heat release rate is critical for understanding how fuel injection methods, fuel types, and operating conditions impact design features such as cylinder geometry, combustion dynamics, and overall engine performance. Figure 6(*b*) depicts the variation in heat release rate with a crank position at full load, highlighting that the WPO20 fuel blend results in a lower heat release rate than the other blends. The HRR values for diesel, WPO20, WPO20 + 30 ppm ZnO, WPO20 + 60 ppm ZnO, WPO20 + 90 ppm ZnO, and WPO20 + 120 ppm ZnO were 35.01 J/deg, 29.78 J/deg, 31.76 J/deg, 32.53 J/deg, 32.65 J/deg, and 33.51 J/deg, respectively. The conventional diesel fuel blend exhibited a superior heat release rate than the other blends. In comparison to diesel, the heat release rate decreased by 14.67% for WPO20, 9.12% for WPO20 + 30 ppm ZnO, 7.06% for WPO20 + 60 ppm ZnO, 6.74% for WPO20 + 90 ppm ZnO, and 4.29% for WPO20 + 30 ppm ZnO. ZnO nanoparticles serve as a catalyst, accelerating the oxidation process and releasing heat more efficiently, resulting in a faster energy release that improves engine performance. Under full-load conditions, WPO20 + 30 ppm ZnO, WPO20 + 60 ppm ZnO, WPO20 + 90 ppm ZnO, and WPO20 + 120 ppm ZnO showed heat release rate increases of 6.66%, 9.18%, 9.68%, and 12.5%, respectively, compared to WPO20. The results showed that the WPO20 + 120 ppm ZnO blend exhibited the highest heat release rate, as the increased ZnO concentration improved fuel oxidation, leading to a faster temperature rise and quicker combustion. These findings align with previous studies, where aluminum oxide nanoparticles were incorporated into fuel blends to enhance thermal conductivity and ignition quality, accelerating fuel combustion and increasing the heat release rate [43].

3.4 Brake-Specific Fuel Consumption. Figure 7(*a*) reveals the effect of different tested fuel samples and load conditions on brake-specific fuel consumption. According to the findings, when engine load increases, BSFC is reduced. Specifically, the BSFC decreases as the load increases because more fuel is needed to operate the engine. At full-load conditions, the BSFC values were 0.235, 0.287, 0.268, 0.259, 0.247, and 0.241 kg/kW-h for the diesel, WPO20, WPO20 + 30 ppm ZnO, WPO20 + 60 ppm ZnO, WPO20 + 90 ppm ZnO, and WPO20 + 120 ppm ZnO blends, respectively. The addition of ZnO nanoparticles to WPO20 blends increases fuel atomization and combustion efficiency, lowering brake-specific fuel consumption. Furthermore, nanoparticles act as oxygen donors, enhancing oxygen availability during combustion and facilitating more complete and efficient fuel burning. When operating at a peak load, the brake-specific fuel consumption increased by 22.12%, 14.04%, 10.21%, 5.1%, and 2.55% for WPO20, WPO20 + 30 ppm ZnO, WPO20 + 60 ppm ZnO, WPO20 + 90 ppm ZnO, and WPO20 + 120 ppm ZnO blends, respectively, compared to conventional diesel. The catalytic efficiency of ZnO nanoparticles improves considerably with higher concentrations, enhancing the combustion process. This improvement reduces BSFC, allowing the engine to deliver the same power output while using less fuel. These results align with earlier research, which indicates that nanoparticle-infused fuel blends achieve lower BSFC than those without nanoparticles, owing to their heightened reactivity [44].

3.5 Brake Thermal Efficiency. Figure 7(*b*) compares brake thermal efficiency across different fuel blends at varying engine loads. The notable increase in BTE at high-load conditions can be attributed to factors such as engine load, speed, and the higher concentration of nanoadditives. These factors enhance heat transfer, reduce combustion delay, and improve combustion efficiency. During peak load conditions, the brake thermal efficiency was observed to be 33.87% for diesel, 30.86% for WPO20, 31.46% for WPO20 + 30 ppm ZnO, 32.02% for WPO20 + 60 ppm ZnO, 32.46% for WPO20 + 90 ppm ZnO, and 33.02% for WPO20 + 120 ppm ZnO. The addition of ZnO nanoparticles to mixed fuel blends improves brake thermal efficiency through multiple mechanisms. The small amount of nanoparticles generates higher

Downloaded from http://asmedigitalcollection.asme.org/energyresourcesrenewable/article-pdf/1/5/051503/7492444/jerta-24-1207.pdf by University of Witwatersrand - Warteweiler Library user on 20 May 2025



Element	Weight %	Atomic %
C	23.93	43.83
O	29.93	35.64
Zn	46.14	20.53
Total	100	

Fig. 5 Characterization of ZnO nanoparticles: (*a*) SEM, (*b*) TEM, and (*c*) EDX

pressures, which increase cylinder pressure during combustion. This pressure increase accelerates combustion and reduces ignition delay, resulting in more efficient energy conversion and enhanced BTE [45]. Compared to diesel, the percentage decreases in BTE were 8.88% for WPO20, 7.11% for WPO20 + 30 ppm ZnO, 5.46% for WPO20 + 60 ppm ZnO, 4.16% for WPO20 + 90 ppm ZnO, and 2.5% for WPO20 + 120 ppm ZnO. Incorporating ZnO nanoparticles into a waste plastic oil blends improves heat transfer, increasing the localized temperature of the fuel–air mixture. This facilitates faster ignition and more complete combustion. The higher temperatures enhance flame propagation, resulting in more thorough combustion and improved energy conversion.

3.6 Carbon Monoxide Emission. Carbon monoxide is released as a result of incomplete combustion, which is caused by insufficient air–fuel mixing. The following factors consider CO formation: oxygen availability, ignition delay, temperature, and spray characteristics. Figure 8(*a*) illustrates the trends in carbon monoxide emissions for different fuel mixtures with respect to engine load. Under maximum load, the CO emissions for the blends were 0.078% for diesel, 0.074% for WPO20, 0.071% for WPO20 + 30 ppm ZnO, 0.068% for WPO20 + 60 ppm ZnO, 0.065% for WPO20 + 90 ppm ZnO, and 0.063% for WPO20 + 120 ppm ZnO. The zinc oxide nanoparticles enhance the combustion process, leading to a more thorough oxidation of carbon into carbon dioxide, reducing carbon monoxide emissions. The WPO20 + 120 ppm ZnO blend demonstrated the most significant reduction in carbon monoxide emissions compared to other fuel blends. At maximum load, carbon monoxide emissions were reduced by 5.1%, 8.97%, 12.82%, 16.6%, and 19.23% for WPO20, WPO20 + 30 ppm ZnO, WPO20 + 60 ppm ZnO, WPO20 + 90 ppm ZnO, and WPO20 + 120 ppm ZnO blends, respectively, compared to diesel. Due to the enhanced fuel oxidation facilitated by the presence of nanoparticles and the additional oxygen they provide, CO emissions have been reduced [46].

3.7 Hydrocarbon Emission. This formation of hydrocarbon emission is attributed to an inadequate supply of oxygen and a reduced oxidation reaction during combustion. The variations in hydrocarbon emissions, as influenced by different load and fuel blends, are shown in Fig. 8(*b*) At maximum load, the HC emissions for the various blends were 76 ppm for diesel, 70 ppm for WPO20, 63 ppm for WPO20 + 30 ppm ZnO, 56 ppm for WPO20 + 60 ppm ZnO, 52 ppm for WPO20 + 90 ppm ZnO, and 45 ppm for WPO20 + 120 ppm ZnO. Using ZnO nanoparticles resulted in enhanced combustion efficiency and reduced hydrocarbon emissions. The WPO20 + 120 ppm ZnO exhibited the most significant decrease in hydrocarbon emissions among the samples tested. At peak load, the hydrocarbon emission decreases for the blends WPO20, WPO20 + 30 ppm ZnO, WPO20 + 60 ppm ZnO, WPO20 + 90 ppm ZnO, and WPO20 + 120 ppm ZnO were 7.89%, 17.11%, 26.32%, 31.58%, and 40.79%, respectively, compared to conventional diesel. An inverse relationship exists between the reduction in HC emissions and the increase in the mass concentration of ZnO nanoparticles. This can be attributed to the beneficial effects of ZnO nanoparticles on the combustion process, such as reduced ignition delay and improved combustion characteristics. Likewise, ZnO nanoparticles may function as catalysts, facilitating more complete combustion and thereby reducing HC emissions [47].

3.8 Smoke Opacity. Smoke formation in internal combustion engines primarily occurs due to incomplete combustion, often caused by poor fuel atomization, overfueling, or a low air–fuel ratio that limits oxygen availability. The smoke opacity of various engine loads and fuel blends is shown in Fig. 8(*c*). Under full conditions, smoke opacity was 77.4% for diesel, 74.4% for WPO20,

Downloaded from http://asmedigitalcollection.asme.org/energyresourcesrenewable/article-pdf/1/5/051503/7492444/jerta-24-1207.pdf by University of Witwatersrand - Warteweiler Library user on 20 May 2025

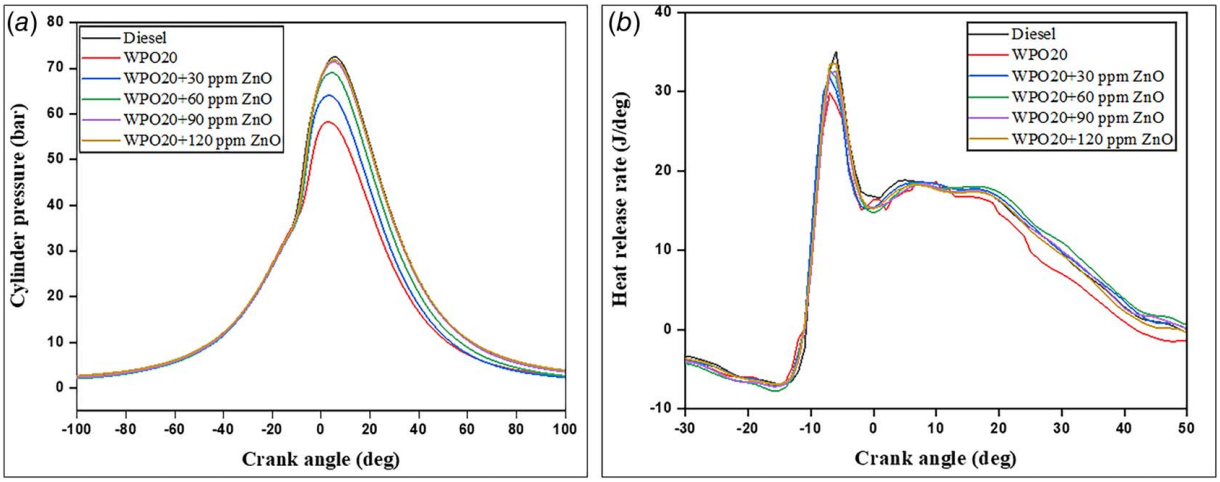


Fig. 6 (*a*) Cylinder pressure and (*b*) heat release rate variations across the crank angle at full load condition

72.3% for WPO20 + 30 ppm ZnO, 70.1% for WPO20 + 60 ppm ZnO, 68.5% for WPO20 + 90 ppm ZnO, and 65.1% for WPO20 + 120 ppm ZnO. The results show that the WPO20 + 120 ppm ZnO blend reduced the most significant smoke opacity compared to the other blends examined. Incorporating ZnO nanoparticles helps reduce smoke opacity by increasing oxygen availability, promoting more complete combustion, and lowering unburned hydrocarbons and particulate matter levels. Smoke opacity at full-load decreased by 3.88%, 6.59%, 9.43%, 11.50%, and 15.89% for the blends WPO20, WPO20 + 30 ppm ZnO, WPO20 + 60 ppm ZnO, WPO20 + 90 ppm ZnO, and WPO20 + 120 ppm ZnO, respectively, relative to diesel. The increased surface area-to-volume ratio and higher cetane number of ZnO nanoparticles promote more complete combustion. Additionally, the higher oxygen content in the fuel blend improves the combustion process, reducing smoke opacity. Furthermore, the elevated sulfur and oxygen content of the nanoparticles in the blend further contribute to lowering smoke opacity [48].

3.9 Nitrogen Oxide Emission. Higher oxygen content and combustion chamber temperatures promote the generation of NO_x. Figure 8(*d*) illustrates the differences in NO_x emissions across different blends and load conditions. Nitrogen oxide emissions progressively increase as engine load tends to rise. The NO_x emissions at full-load conditions were observed in diesel for 1497 ppm, 1501 ppm for WPO20, 1511 ppm for WPO20 + 30 ppm ZnO, 1528 ppm for WPO20 + 60 ppm ZnO, 1532 ppm for WPO20 + 90 ppm ZnO, and 1542 ppm for WPO20 + 120 ppm ZnO. When comparing the NO_x emissions of the various tested fuels, the WPO20 + 120 ppm ZnO blend exhibited the highest levels. At maximum load, the increase in nitrogen oxide emissions compared to pure diesel was 0.27% for WPO20, 0.94% for WPO20 + 30 ppm ZnO, 2.07% for WPO20 + 60 ppm ZnO, 2.34% for WPO20 + 90 ppm ZnO, and 3.01% for WPO20 + 120 ppm ZnO. The maximum nitrogen oxide emission was reported for WPO20 + 120 ppm ZnO. Incorporating zinc oxide nanoparticles into WPO20 blends enhances combustion completeness by increasing oxygen content. However, this raises cylinder temperatures, leading to higher nitrogen oxide emissions. Additionally, including nanoparticle blends extends the ignition delay, promoting faster-premixed combustion. As a result, higher combustion temperatures are reached, further increasing nitrogen oxide emissions [49].

4 Tribological Behaviors

This study evaluates waste plastic oil's tribological performance by incorporating ZnO nanoparticles at 30, 60, 90, and 120 ppm concentrations, using a four-ball tribometer to assess the results. The small size of ZnO nanoparticles allows them to effectively penetrate the contact points between surfaces, enhancing lubrication and reducing wear. The comprehensive findings of this assessment are detailed in the following section.

4.1 Coefficient of Friction. Figure 9(*a*) illustrates the variance in the coefficient of friction for various fuel blends. The coefficient of friction for the tested samples, including diesel, WPO20, WPO20 + 30 ppm ZnO, WPO20 + 60 ppm ZnO, WPO20 + 90 ppm ZnO,

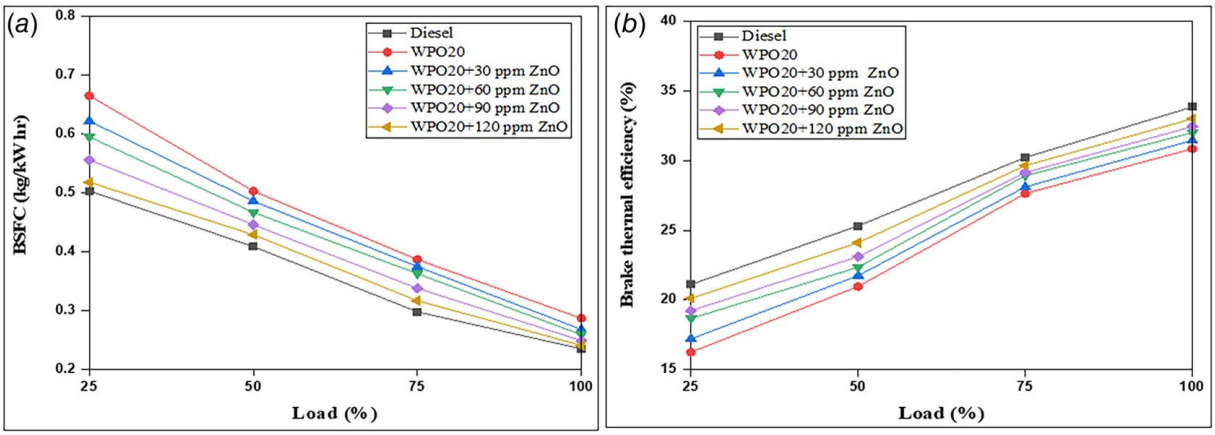


Fig. 7 (*a*) BSFC and (*b*) BTE variation with load

Downloaded from http://asmedigitalcollection.asme.org/energyresourcesrenewable/article-pdf/1/5/051503/7492444/jerta-24-1207.pdf by University of Witwatersrand - Warteweiler Library user on 20 May 2025

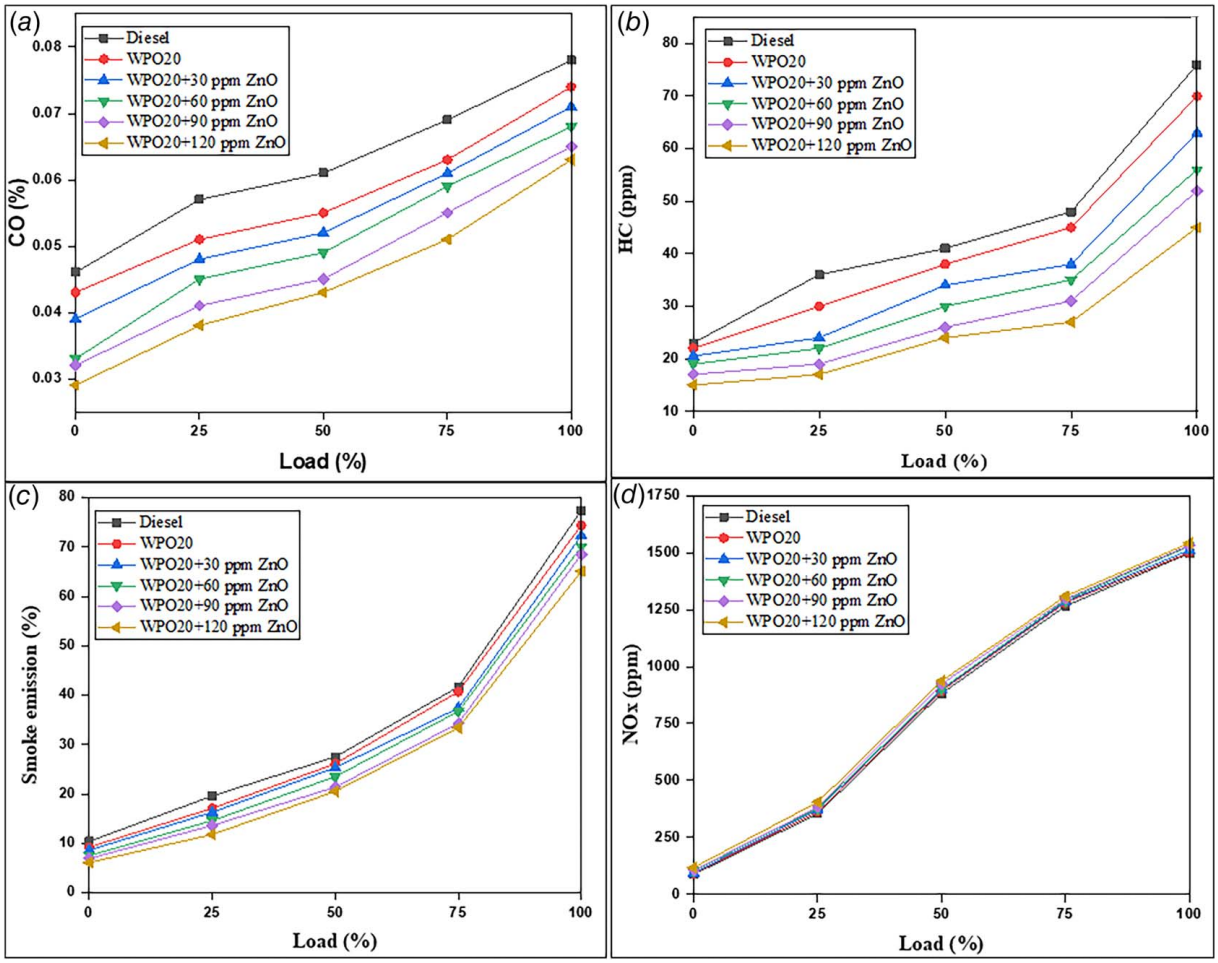


Fig. 8 (*a*) CO, (*b*) HC, (*c*) smoke, and (*d*) NO_x variation with load

and WPO20 + 120 ppm ZnO, were found to be 0.08633, 0.08321, 0.07634, 0.07182, 0.06972, and 0.06591, respectively. Compared to other test fuel samples, diesel fuel exhibits a maximum coefficient of friction. In comparison to pure diesel, the coefficient of friction was reduced by 3.61% for WPO20, 11.59% for WPO20 + 30 ppm ZnO, 16.79% for WPO20 + 60 ppm ZnO, 19.25% for WPO20 + 90 ppm ZnO, and 23.69% for WPO20 + 120 ppm ZnO. The fatty acids in waste plastic oil contribute to its superior lubrication properties by helping form a stable lubricating film. Meanwhile, waste plastic oil extracted through the pyrolysis process typically contains residual organic materials, including fatty acids, which enhance its lubrication properties compared to conventional petroleum-based oils. Furthermore, it has been shown that adding ZnO nanoparticles enhances the fuel's lubricating properties. Due to their small size and spherical shape, ZnO nanoparticles can penetrate surface imperfections, reducing the contact area between sliding surfaces and thereby lowering friction. Increasing the ZnO concentration further decreases the coefficient of friction by providing more nanoparticles, which help create a smoother and more lubricated interface. Similar findings have been reported in other studies. For instance, incorporating a GO/CeO_2 nanohybrid material into rapeseed oil resulted in a 36.5% decrease in COF with the addition of 0.1% GO/CeO_2 compared to neat rapeseed oil [50]. In another study, adding CuO and SiO_2 nanoparticles to coconut oil significantly decreased the COF by 93.75% and 93.25%, respectively [51].

4.2 Flash Temperature Parameter. The flash temperature parameter helps predict the risk of lubricant breakdown and potential failure of lubricated surfaces under high stress. The flash temperature parameter exhibits an inverse relationship with the wear scar diameter: a lower value may cause lubrication film breakdown, whereas a higher value enhances lubrication efficiency. The flash temperature parameter for the various tested fuels is displayed in Fig. 9(*b*). Based on the outcomes, the flash temperature parameter, the values observed for the samples diesel, WPO20, WPO20 + 30 ppm ZnO, WPO20 + 60 ppm ZnO, WPO20 + 90 ppm ZnO, and WPO20 + 120 ppm ZnO were 51.94 °C, 54.82 °C, 63.95 °C, 67.94 °C, 81.07 °C, and 86.99 °C, respectively. The highest concentrations of ZnO in WPO20 exhibited higher flash temperature parameters. The findings indicate that ZnO nanoparticles in waste plastic oil blends enhance fuel thermal stability, improving fuel performance at elevated temperatures. Compared to diesel fuel, the flash temperature parameter was increased by 5.54% for WPO20, 23.12% for WPO20 + 30 ppm ZnO, 30.8% for WPO20 + 60 ppm ZnO, 56.08% for WPO20 + 90 ppm ZnO, and 67.48% for WPO20 + 120 ppm ZnO.

4.3 Wear Scar Diameter. The variations in wear scar diameter for the different fuel blends are shown in Fig. 9(*c*). According to graph, wear scar diameters for the samples diesel, WPO20, WPO20 + 30 ppm ZnO, WPO20 + 60 ppm ZnO, WPO20 + 90 ppm ZnO, and WPO20 + 120 ppm ZnO were 0.8324 mm, 0.7984 mm, 0.7152 mm, 0.6849 mm, 0.6037 mm, and 0.5741 mm, respectively. Experimental results indicated that the pure diesel blend had a significantly larger wear scar diameter than the WPO20 and WPO20 blends containing nanoparticles. The wear scar diameter reductions for WPO20, WPO20 + 30 ppm ZnO, WPO20 + 60 ppm ZnO, WPO20 + 90 ppm ZnO, and WPO20 +

Downloaded from http://asmedigitalcollection.asme.org/energyresourcesrenewable/article-pdf/1/5/051503/7492444/jerta-24-1207.pdf by University of Witwatersrand - Warteweiler Library user on 20 May 2025

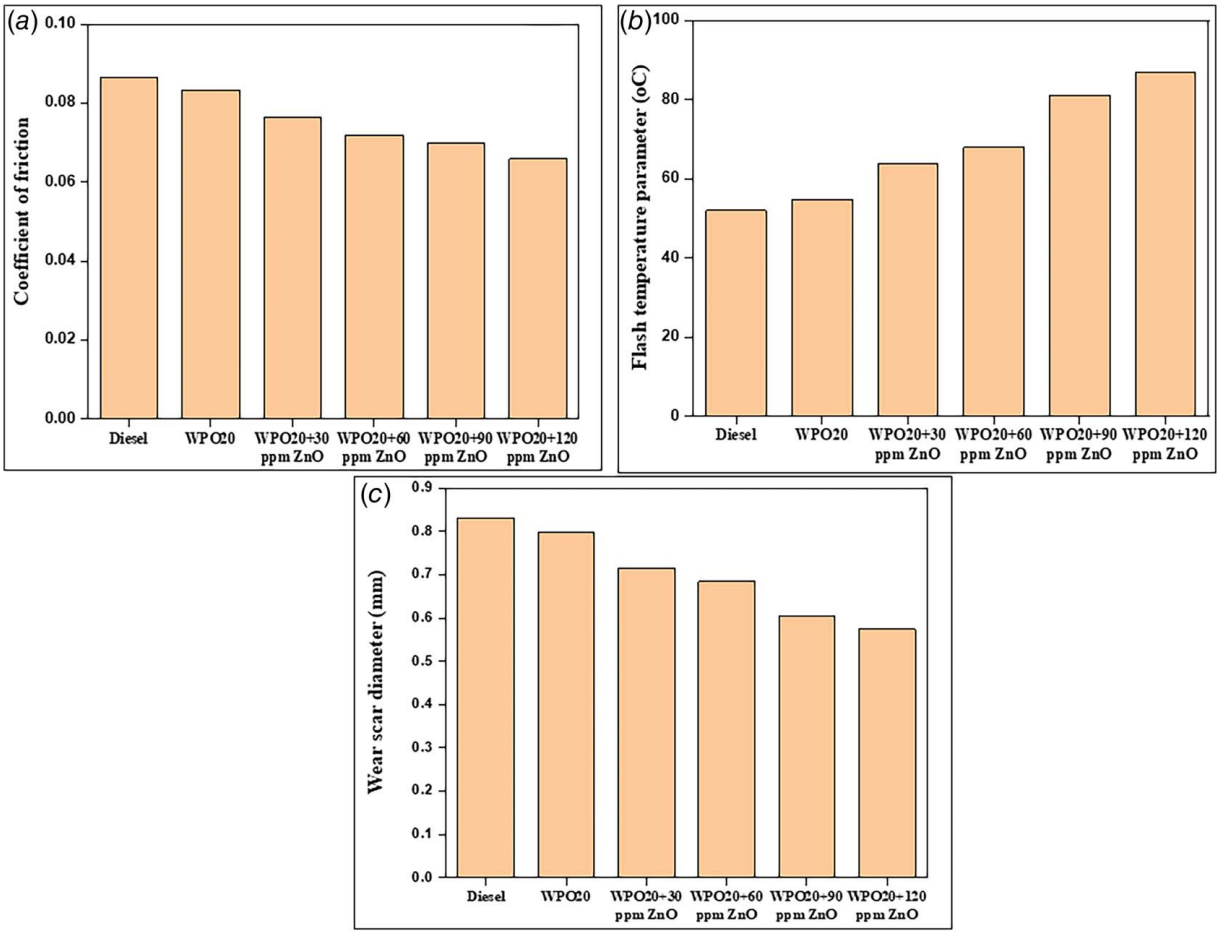


Fig. 9 (*a*) COF, (*b*) FTP, and (*c*) WSD variation with different fuel blends

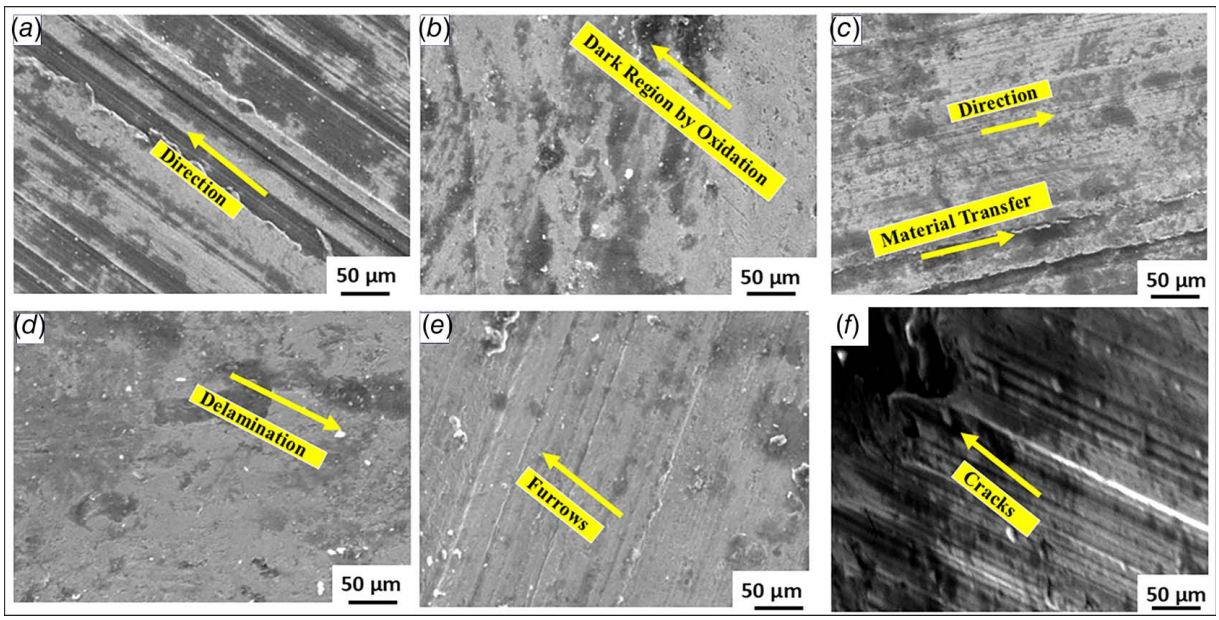


Fig. 10 SEM characterization of wear scar surface morphologies in steel balls lubricated by (*a*) WPO20, (*b*) WPO20 + 30 ppm of ZnO, (*c*) WPO20 + 60 ppm ZnO, (*d*) WPO20 + 90 ppm ZnO, (*e*) WPO20 + 120 ppm ZnO, and (*f*) diesel

Downloaded from http://asmedigitalcollection.asme.org/energyresourcesrenewable/article-pdf/1/5/051503/7492444/jerta-24-1207.pdf by University of Witwatersrand - Warteweiler Library user on 20 May 2025

120 ppm ZnO blends were 4.08%, 14.07%, 17.73%, 27.56%, and 31.05%, respectively, in comparison to diesel fuel. The findings indicated that blends with higher nanoparticle concentrations reduced the wear scar diameter, as the tiny ZnO nanoparticles filled surface imperfections, thereby minimizing wear [52]. Furthermore, ZnO nanoparticles exhibit strong antiwear properties as a result of their ability to form protective tribofilms under sliding conditions. Compared to WPO20, the wear scar diameter was reduced by 10.42% for WPO20 + 30 ppm ZnO, 14.21% for WPO20 + 60 ppm ZnO, 24.39% for WPO20 + 90 ppm ZnO, and 28.09% for WPO20 + 120 ppm ZnO fuel blends. These tribofilms help decrease the wear scar by preventing metal-on-metal contact, while ZnO's high thermal conductivity efficiently absorbs the heat produced during friction. As a result, higher concentrations of ZnO in waste plastic oil blends provide superior surface protection, progressively reducing the wear scar diameter. Other researchers have reported similar results, showing that the analysis of CuO nanoparticles in castor oil resulted in an almost 28.3% reduction in wear scar diameter [53].

4.4 Scanning Electron Microscopic Analysis. Scanning electron microscopy revealed several distinct features on the worn surfaces of the steel balls tested using the four-ball tribometer. Figures 10(*a*)–10(*f*) show SEM images of the worn surface of the tested balls and depict the wear scar diameter for the different fuel blends. The presence of ZnO nanoparticles in the WPO20 blend formed a protective film on the surface asperities, preventing direct friction and enhancing the ball surface. This resulted in a smoother surface compared to the WPO20 and diesel samples. Figures 10(*a*) and 10(*f*) show that the worn surface exhibits noticeable oxidation in the SEM images of WPO20 and diesel, appearing as dark patches scattered across the surface. These dark regions indicate the presence of oxidation. The SEM images indicated more severe wear, delamination, deep furrows, and pits compared to WPO20 blends with nanoparticles. The lack of nanoparticles implies increased surface damage, possibly due to inadequate lubrication and increased frictional forces. In contrast, Figs. 10(*b*)–10(*e*) show that the SEM images of worn surfaces with ZnO nanoparticle blends exhibit fewer deep furrows and pits, indicating enhanced surface protection and reduced wear. There is a protective tribofilm formed by the ZnO nanoparticles that improve lubrication and reduces direct contact between the steel surfaces, which contributes to the observed reduction in wear. The SEM analysis of the WPO20 with nanoparticle samples confirms fewer pits and cracks, indicating improved surface integrity under load conditions. The results demonstrate that nanoparticles in waste plastic oil significantly reduce wear, as shown by a smoother, less-damaged surface than diesel and WPO20.

5 Conclusion

This study comprehensively examined the impact of zinc oxide nanoparticles on the performance, combustion, and emission properties of a diesel engine fueled by waste plastic oil. The experimental findings provide valuable insights into how ZnO nanoparticles influence engine characteristics. Additionally, a four-ball tribometer was used to analyze the tribological characteristics. Key conclusions from the study are as follows:

- SEM, TEM, and EDX analyses revealed the morphological features of ZnO nanoparticles.
- Among the tested fuel samples, the diesel fuel blend exhibited the maximum cylinder pressure and heat release rate, achieving 72.47% and 35.01 J/deg, respectively, compared to other blends at maximum load conditions. In comparison, the WPO20 + 120 ppm ZnO showed a 23.53% increase in cylinder pressure and a 12.5% improvement in heat release rate relative to WPO20. This enhancement is attributed to the catalytic effect of ZnO nanoparticles, which improved the fuel's thermal conductivity and facilitated more efficient combustion. Consequently, this led to better energy release and pressure generation, particularly under maximum load conditions.
- Among the evaluated fuel samples, the diesel fuel blend demonstrated the lowest brake-specific fuel consumption at 0.235 kg/kW-h, highlighting its superior fuel economy and high brake thermal efficiency of 33.87%. In comparison, the WPO20 + 120 ppm ZnO blend surpassed the standard WPO20 blend by achieving a 6.54% increase in BTE and a 16.02% reduction in BSFC. These improvements are attributed to the catalytic effects of ZnO nanoparticles, which enhanced combustion efficiency by promoting better atomization and fuel–air mixing, leading to optimized energy utilization.
- At maximum load, the blend of WPO20 + 120 ppm ZnO demonstrated a 19.23% reduction in carbon monoxide emissions. This improvement can be attributed to the catalytic properties of ZnO nanoparticles, which promote more complete combustion during engine operation. Hydrocarbon emissions dropped by 40.79%, reflecting improved combustion efficiency and reduced unburnt fuel in the exhaust, while smoke opacity decreased by 15.89%, likely due to minimized soot formation compared to pure diesel.
- However, a slight 3.01% increase in nitrogen oxide emissions was observed, primarily resulting from higher combustion temperatures and increased oxygen availability associated with biodiesel combustion compared to conventional diesel under peak load.
- Tribological evaluations using a four-ball tribometer demonstrated significant improvements in the WPO20 + 120 ppm ZnO. The coefficient of friction was reduced by 23.69%, indicating improved lubrication properties due to the ZnO nanoparticles forming a protective film on the contacting surfaces. Additionally, the wear scar diameter decreased by 31.05%, highlighting the enhanced antiwear characteristics of the nanoparticle-enriched blend. Furthermore, the flash temperature parameter improved by 67.48%, reflecting superior thermal resistance and surface protection under high-temperature conditions compared to conventional diesel.
- SEM analysis revealed that the diesel and WPO20 blends exhibited more severe wear, surface damage, oxidation, and delamination, indicating poor tribological performance. In contrast, the WPO20 + 120 ppm ZnO blend showed smoother surfaces with less wear and minimal signs of damage, confirming the protective and lubricating effects of ZnO nanoparticles.

Despite the increase in NO_x emissions, ZnO nanoparticles notably improved engine performance, combustion efficiency, and emission reductions when blended with waste plastic oil. This study kept the engine configuration unchanged. Future research should investigate the effects of modifying the injection nozzle design and adjusting the injection pressure. Moreover, applying coatings to the piston and assessing the resulting engine performance could offer valuable insights. Long-term studies are also needed to evaluate the impact of engine wear.

Conflict of Interest

There are no conflicts of interest.

Data Availability Statement

The datasets generated and supporting the findings of this article are obtainable from the corresponding author upon reasonable request.

Nomenclature

Al_2O_3 = aluminum oxide
ASTM = American society for testing and materials

Downloaded from http://asmedigitalcollection.asme.org/energyresourcesrenewable/article-pdf/1/5/051503/7492444/jerta-24-1207.pdf by University of Witwatersrand - Warteweiler Library user on 20 May 2025

BTE = brake thermal efficiency
BSFC = brake-specific fuel consumption
CeO_2 = cerium oxide
CO = carbon monoxide
COF = coefficient of friction
CuO = copper oxide
EDX = energy-dispersive X-ray analysis
FTP = flash temperature parameter
GNP = graphene nanoplatelet
hBN = hexagonal boron nitride
HC = hydrocarbon
kg = kilogram
kW = kilowatt
La_2O_3 = lanthanum oxide
MgO = magnesium oxide
MT = metric ton
NO_x = nitrogen oxides
O = oxygen
PO = plastic oil
PPO = plastic pyrolysis oil
ppm = parts per million
rpm = revolutions per minute
SEM = scanning electron microscope
TEM = transmission electron microscope
TiO_2 = titanium oxide
WPO = waste plastic oil
WPO20 = 20% waste plastic oil
WPO20 + 30 ppm ZnO = 80% diesel + 20% waste plastic oil + 30 ppm zinc oxide
WPO20 + 60 ppm ZnO = 80% diesel + 20% waste plastic oil + 60 ppm zinc oxide
WPO20 + 90 ppm ZnO = 80% diesel + 20% waste plastic oil + 90 ppm zinc oxide
WPO20 + 120 ppm ZnO = 80% diesel + 20% waste plastic oil + 120 ppm zinc oxide
WS_2 = tungsten disulfide
Zn = zinc
ZnO = zinc oxide

References

[1] Prabhu, L., Dhanalakshmi, K., Alahmadi, T. A., Alharbi, S. A., Sołowski, G., and Veeman, D., 2023, "How Do Microalgae Biodiesel Blends Affect the Acoustic and Vibration Characteristics of the Direct Injection Diesel Engine: An Experimental Examination," ASME J. Energy Resour. Technol., **145**(11), p. 112101.

[2] Qenawy, M., Khalaf, M., Wang, J., Tian, J., Zuo, L., Mustafa, H. M. M., and Esmail, M. F. C., 2024, "Performance and Emission of Extracted Biodiesel From Mixed Jatropha-Castor Seeds," Fuel, **357**, p. 130060.

[3] Praveenkumar, T. R., Rath, B., Devanesan, S., Alsahi, M. S., Jhanani, G. K., Gemede, H. F., Solowski, G., and Daniel, F., 2023, "Performance and Emission Characteristics for Karanja Biodiesel Blends Assisted With Green Hydrogen Fuel and Nanoparticles," ASME J. Energy Resour. Technol., **145**(11), p. 112702.

[4] OECD, 2022, *Global Plastics Outlook: Economic Drivers, Environmental Impacts and Policy Options*, OECD, Paris.

[5] Nimita Jebaranjitham, J., Selvan Christyraj, J. D., Prasannan, A., Rajagopalan, K., Chelladurai, K. S., and Gnanaraja, J. K. J. S., 2022, "Current Scenario of Solid Waste Management Techniques and Challenges in Covid-19—A Review," Heliyon, **8**(7), p. e09855.

[6] Saha, D., Roy, B., and Kundu, P. P., 2024, "Influence of Injection Timing Variation on Combustion-Emission-Performance Aspects of Emulsified Plastic Oil-Run Compression Ignition Engine," J. Energy Resour. Technol, **146**(9), p. 091201.

[7] Anand, T., and Debbarma, S., 2024, "Experimental Analysis of Hydrogen Enrichment in Waste Plastic Oil Blends for Dual-Fuel Common Rail Direct Injection Diesel Engines," ASME J. Energy Resour. Technol., **146**(1), p. 012302.

[8] El-Seesy, A. I., Nour, M., Hassan, H., Elfasakhany, A., He, Z., and Mujtaba, M. A., 2021, "Diesel-Oxygenated Fuels Ternary Blends With Nano Additives in Compression Ignition Engine: A Step Towards Cleaner Combustion and Green Environment," Case Stud. Therm. Eng., **25**, p. 100911.

[9] Kalita, P., Basumatary, B., Saikia, P., Das, B., and Basumatary, S., 2022, "Biodiesel as Renewable Biofuel Produced via Enzyme-Based Catalyzed Transesterification," Energy Nexus, **6**, p. 100087.

[10] Simbi, I., Aigbe, U. O., Oyekola, O. O., and Osibote, O. A., 2022, "Chemical and Quality Performance of Biodiesel and Petrol Blends," Energy Convers. Manag.: X., **15**, p. 100256.

[11] Tamilselvan, P., Nallusamy, N., and Rajkumar, S., 2017, "A Comprehensive Review on Performance, Combustion and Emission Characteristics of Biodiesel Fuelled Diesel Engines," Renew. Sustain. Energy Rev., **79**, pp. 1134–1159.

[12] Sobotowski, R. A., Porter, B. C., and Pilley, A. D., 1991, "The Development of a Novel Variable Compression Ratio, Direct Injection Diesel Engine," SAE Trans., **100**, pp. 776–792.

[13] Yamaki, Y., Mori, K., Kamikubo, H., Kohketsu, S., Mori, K., and Kato, T., 1994, "Application of Common Rail Fuel Injection System to a Heavy Duty Diesel Engine," SAE Trans., pp. 1977–1988.

[14] Khond, V. W., and Kriplani, V. M., 2016, "Effect of Nanofluid Additives on Performances and Emissions of Emulsified Diesel and Biodiesel Fueled Stationary CI Engine: A Comprehensive Review," Renew. Sustain. Energy Rev., **59**, pp. 1338–1348.

[15] Shaafi, T., Sairam, K., Gopinath, A., Kumaresan, G., and Velraj, R., 2015, "Effect of Dispersion of Various Nanoadditives on the Performance and Emission Characteristics of a CI Engine Fuelled With Diesel, Biodiesel and Blends—A Review," Renew. Sustain. Energy Rev., **49**, pp. 563–573.

[16] Saxena, V., Kumar, N., and Saxena, V. K., 2017, "A Comprehensive Review on Combustion and Stability Aspects of Metal Nanoparticles and Its Additive Effect on Diesel and Biodiesel Fuelled CI Engine," Renew. Sustain. Energy Rev., **70**, pp. 563–588.

[17] Soudagar, M. E. M., Nik-Ghazali, N. N., Kalam, M. A., Badruddin, I. A., Banapurmath, N. R., and Akram, N., 2018, "The Effect of Nano-Additives in Diesel-Biodiesel Fuel Blends: A Comprehensive Review on Stability, Engine Performance and Emission Characteristics," Energy Convers. Manage., **178**, pp. 146–177.

[18] Nithya, S., Jeyaseelan, G. A. C., Ali Alharbi, S., Alfarraj, S., and Jhanani, G. K., 2023, "Prediction of Waste Chicken Fat Biodiesel Blends as the Potential Substitute for the Diesel Engine With Oxygenated Additives," J. Energy Resour. Technol, **145**(9), p. 091301.

[19] Wu, L., Zhang, Y., Yang, G., Zhang, S., Yu, L., and Zhang, P., 2016, "Tribological Properties of Oleic Acid-Modified Zinc Oxide Nanoparticles as the Lubricant Additive in Poly-Alpha Olefin and Diisooctyl Sebacate Base Oils," RSC Adv., **6**(74), pp. 69836–69844.

[20] Fouda, A. N., El Basaty, A. B., and Eid, E. A., 2016, "Photo-Response of Functionalized Self-Assembled Graphene Oxide on Zinc Oxide Heterostructure to UV Illumination," Nanoscale Res. Lett., **11**(1), pp. 1–8.

[21] Soundararajan, G., Bibin, C., Kumar, A., Arunkumar, S., Rajesh, K., Devarajan, Y., and Mishra, R., 2025, "Synergistic Effects of Graphene Quantum Dot Additives in Waste Plastic Oil Blends: Combustion Stability and Emission Reductions Analysis," Results Eng., **25**, p. 104130.

[22] Uslu, S., 2025, "An Additional Value for the Disposed Wastes: An Experimental and RSM Optimization Study Based on the Enhancement of Waste Plastic Oil/Diesel Fuel Blend With Optimum B_2O_3 Nanoparticles for Cleaner Emissions," J. Energy Inst., **119**, p. 102013.

[23] Suhel, A., Rahim, N. A., Rahman, M. R. A., Ahmad, K. A. B., Khan, U., Teoh, Y. H., and Abidin, N. Z., 2023, "Impact of ZnO Nanoparticles as Additive on Performance and Emission Characteristics of a Diesel Engine Fueled With Waste Plastic Oil," Heliyon, **9**(4), p. e14782.

[24] Sachuthananthan, B., Krupakaran, R. L., and Balaji, G., 2021, "Exploration on the Behaviour Pattern of a DI Diesel Engine Using Magnesium Oxide Nano Additive With Plastic Pyrolysis Oil as Alternate Fuel," Int. J. Ambient Energy, **42**(6), pp. 701–712.

[25] Sathyamurthy, R., Salman, M. S., Vijayabalan, P., Sundar, S. P., and Dharmaraj, V., 2022, "Analysis of DI CI Engine Fueled With Neat Plastic Oil and Titanium Oxide Nanomaterial as an Additive," Mater. Today: Proc., **50**, pp. 560–564.

[26] Sundar, S. P., Palanimuthu, V., Sathyamurthy, R., Hemalatha, D., Kumar, R. S., Bharathwaaj, R., Vasanthaseelan, S., and Chamkha, A., 2022, "Feasibility Study of Neat Plastic Oil With TiO_2 Nanoadditive as an Alternative Fuel in Internal Combustion Engine," J. Therm. Anal. Calorim., **147**(3), pp. 2567–2578.

[27] Bharathy, S., Gnanasikamani, B., and Radhakrishnan Lawrence, K., 2019, "Investigation on the Use of Plastic Pyrolysis Oil as Alternate Fuel in a Direct Injection Diesel Engine With Titanium Oxide Nanoadditive," Environ. Sci. Pollut. Res., **26**(10), pp. 10319–10332.

[28] Thomas, T. J., Thangapandian, N., Sakthivel, D., Mohideen, S. M. S. F., Basha, S., Brindhadevi, K., and Ramya, G., 2022, "Experimental Analysis of CI Engine Using Pyrolyzed Plastic Oil Blended With Alumina Nano Additive," Fuel, **312**, p. 122929.

[29] Sachuthananthan, B., Vinoth, R., Reddy, D. R., Bandari, V., and Anusha, P., 2021, "Environmental Impact on the Use of Diesel Waste Plastic Oil Nano-Additive Blends in a DI Diesel Engine," Int. J. Nanotechnol., **18**(11–12), pp. 990–1006.

[30] Yaqoob, H., Heng, T. Y., and Tebal, N., 2022, "Friction and Wear Characteristics of Tire Pyrolysis Oil," ASME J. Tribol., **32**, pp. 56–68.

[31] Baskar, S., Arumugam, S., Sriram, G., and Sistla, V. S. S. S., 2019, "Tribological Investigation of Waste Plastic Oil-Based Methyl Ester Blended Synthetic Lubricant Using Four-Ball Tribometer," Advances in Materials and Manufacturing Engineering: Select Proceedings of ICMME 2019, Kanchipuram, India, Mar. 21–22, pp. 587–593.

[32] Verma, A., Jiang, W., Abu Safe, H. H., Brown, W. D., and Malshe, A. P., 2008, "Tribological Behavior of Deagglomerated Active Inorganic Nanoparticles for Advanced Lubrication," Tribol. Trans., **51**(5), pp. 673–678.

[33] Peña-Parás, L., Taha-Tijerina, J., Garza, L., Maldonado-Cortés, D., Michalczewski, R., and Lapray, C., 2015, "Effect of CuO and Al_2O_3 Nanoparticle Additives on the Tribological Behavior of Fully Formulated Oils," Wear, **332**, pp. 1256–1261.

Downloaded from http://asmedigitalcollection.asme.org/energyresourcesrenewable/article-pdf/1/5/051503/7492444/jerta-24-1207.pdf by University of Witwatersrand - Warteweiler Library user on 20 May 2025

[34] Nallasamy, P., Saravanakumar, N., Nagendran, S., Suriya, E. M., and Yashwant, D., 2015, "Tribological Investigations on MoS_2-Based Nanolubricant for Machine Tool Slideways," ImechE, **229**(5), pp. 559–567.
[35] Loo, D. L., Teoh, Y. H., How, H. G., Le, T. D., Nguyen, H. T., Rashid, T., Pottmaier, D., and Sher, F., 2023, "Effect of Nanoparticles Additives on Tribological Behaviour of Advanced Biofuels," Fuel, **334**, p. 126798.
[36] Sikdar, S., Rahman, M. H., Ralls, A. M., and Menezes, P. L., 2023, "Enhancement in Tribological Performance of Plastic Oil by Solid Lubricant Additives," Lubr. Sci., **35**(6), pp. 385–458.
[37] Sikdar, S., and Menezes, P. L., 2024, "The Role of Functionalized CuO Additive in Enhancing Tribological Performance of Plastic Oil Lubricant," Lubr. Sci., **37**(2), pp. 117–188.
[38] Sikdar, S., and Menezes, P. L., 2024, "Enhancing Lubrication Performance of Plastic Oil Lubricant With Oleic Acid-Functionalized Graphene Nanoplatelets and Hexagonal Boron Nitride Solid Lubricant Additives," Lubricants, **12**(7), p. 251.
[39] Burra, K. R. G., Sahin, M., Zheng, Y., and Gupta, A. K., 2024, "Near-Critical CO_2-Assisted Liquefaction-Extraction of Biomass and Wastes to Fuels and Value-Added Products," J. Energy Resour. Technol, **146**(1), p. 011801.
[40] Lee, X. J., Ong, H. C., Gan, Y. Y., Chen, W. H., and Mahlia, T. M. I., 2020, "State of Art Review on Conventional and Advanced Pyrolysis of Macroalgae and Microalgae for Biochar, Bio-Oil and Bio-Syngas Production," Energy Convers. Manage., **210**, p. 112707.
[41] Ağbulut, U., and Sarıdemir, S., 2021, "A General View to Converting Fossil Fuels to Cleaner Energy Source by Adding Nanoparticles," Int. J. Ambient Energy, **42**(13), pp. 1569–1574.
[42] El-Adawy, M., 2023, "Effects of Diesel-Biodiesel Fuel Blends Doped With Zinc Oxide Nanoparticles on Performance and Combustion Attributes of a Diesel Engine," Alex. Eng. J., **80**, pp. 269–281.
[43] Venu, H., and Appavu, P., 2020, "Al_2O_3 Nano Additives Blended Polanga Biodiesel as a Potential Alternative Fuel for Existing Unmodified DI Diesel Engine," Fuel, **279**, p. 118518.
[44] Karthikeyan, T., and Alwarsamy, T., 2019, "Effects of Copper Oxide Nanoparticle Addition in Diesel and Biodiesel Blends on the Performance and Emission Characteristics of a Diesel Engine," Int. J. Res. Appl. Sci. Eng. Technol., **7**(4), pp. 156–161.
[45] Annamalai, M., Dhinesh, B., Nanthagopal, P., SivaramaKrishnan, P., Isaac JoshuaRamesh Lalvani, J., Parthasarathy, M., and Annamalai, K., 2016, "An Assessment on Performance, Combustion and Emission Behavior of a Diesel Engine Powered by Ceria Nanoparticle Blended Emulsified Biofuel," Energy Convers. Manage., **123**, pp. 372–380.
[46] Ashok, B., Nanthagopal, K., Mohan, A., Johny, A., and Tamilarasu, A., 2017, "Comparative Analysis on the Effect of Zinc Oxide and Ethanox as Additives With Biodiesel in CI Engine," Energy, **140**, pp. 352–364.
[47] Karthikeyan, S., Elango, A., and Prathima, A., 2014, "Diesel Engine Performance and Emission Analysis Using Canola Oil Methyl Ester With the Nano Sized Zinc Oxide Particles," Indian J. Eng. Mater. Sci., **21**, pp. 83–87.
[48] Deepak Kumar, T., Sameer Hussain, S., and Ramesha, D. K., 2020, "Effect of a Zinc Oxide Nanoparticle Fuel Additive on the Performance and Emission Characteristics of a CI Engine Fuelled With Cotton Seed Biodiesel Blends," Mater. Today: Proc., **26**, pp. 2374–2378.
[49] Soudagar, M. E. M., Nik-Ghazali, N. N., Kalam, M. A., Badruddin, I. A., Banapurmath, N. R., Ali, M. A. B., Kamangar, S., Cho, H. M., and Akram, N., 2020, "An Investigation on the Influence of Aluminium Oxide Nano-Additive and Honge Oil Methyl Ester on Engine Performance, Combustion and Emission Characteristics," Renew. Energy, **146**, pp. 2291–2307.
[50] Qiu, S., Chen, B., Yang, B., Dong, W., Tong, Y., Li, J., Xu, J., Zhang, L., and Li, C., 2023, "Facile Construction of Graphene Oxide/CeO_2 Nanohybrid for Enhancing Tribological Properties of Green Rapeseed Oil," Colloids Surf. A: Physicochem. Eng. Asp., **676**, p. 132248.
[51] Cortes, V., and Ortega, J. A., 2019, "Evaluating the Rheological and Tribological Behaviors of Coconut Oil Modified With Nanoparticles as Lubricant Additives," Lubricants, **7**(9), p. 76.
[52] Luo, T., Wei, X., Huang, X., Huang, L., and Yang, F., 2014, "Tribological Properties of Al_2O_3 Nanoparticles as Lubricating Oil Additives," Ceram. Int., **40**(5), pp. 7143–7149.
[53] Gupta, R. N., and Harsha, A. P., 2018, "Tribological Study of Castor oil With Surface-Modified CuO Nanoparticles in Boundary Lubrication," Ind. Lubr. Tribol., **70**(4), pp. 700–710.

Downloaded from http://asmedigitalcollection.asme.org/energyresourcesrenewable/article-pdf/1/5/051503/7492444/jerta-24-1207.pdf by University of Witwatersrand - Warteweiler Library user on 20 May 2025